Kinetics of the NCO + HCNO Reaction†

Wenhui Feng and John F. Hershberger*

Department of Chemistry and Molecular Biology, North Dakota State University, Fargo, North Dakota 58105

Received: September 15, 2006; In Final Form: October 25, 2006

The kinetics of the NCO + HCNO reaction were studied using infrared diode laser absorption spectroscopy. The total rate constant was measured to be $k_1 = (1.58 \pm 0.20) \times 10^{-11}$ cm^3 molecule^{-1} s^{-1} at 298 K. After detection of products and consideration of secondary chemistry (primarily O + HCNO and CN + HCNO), we conclude that NO + CO + HCN is the major product channel ($\varphi = 0.92 \pm 0.04$), with a minor contribution ($\varphi = 0.04 \pm 0.02$) from CO_2 + HCNN.

1. Introduction

Fulminic acid, HCNO, is an important intermediate in NO-reburning process for the reduction of NO_x pollutants from fossil fuel combustion emissions.[1] HCNO is formed primarily from acetylene oxidation followed by the HCCO + NO reaction. The chemistry of HCNO is of great interest in the overall NO-reburning mechanism. In our laboratory, we have previously studied the kinetics of the OH + HCNO and CN + HCNO reactions.[2,3] In this paper, we present a study of the kinetics of the reaction HCNO with the NCO radical. NCO is an important intermediate in several combustion environments, including the RAPRENO$_x$ process for reducing NO_x emissions.[4−6] The title reaction has several thermodynamically possible product channels:

$$\mathrm{NCO + HCNO \rightarrow NO + CO + HCN} \qquad \Delta H_{298}{}^0 = -183.69 \text{ kJ/mol} \quad (1a)$$

$$\rightarrow \mathrm{CO_2 + HCNN} \qquad \Delta H_{298}{}^0 = -232.31 \text{ kJ/mol} \quad (1b)$$

$$\rightarrow \mathrm{CO + HCO + N_2} \qquad \Delta H_{298}{}^0 = -365.62 \text{ kJ/mol} \quad (1c)$$

$$\rightarrow \mathrm{N_2O + HCCO} \qquad \Delta H_{298}{}^0 = -37.99 \text{ kJ/mol} \quad (1d)$$

Thermochemical information has been obtained from NIST-JANAF standard tables[7] as well as other references for the heats of formation of NCO,[8] HCNO,[8] HCNN,[9] and HCCO.[10]

2. Experimental Section

NCO radicals were generated by 248-nm excimer laser photolysis of ICN/O_2 mixtures, using a Compex 200 Excimer laser:

$$\mathrm{ICN} + h\nu\ (248 \text{ nm}) \rightarrow \mathrm{CN + I} \quad (2)$$

$$\mathrm{CN + O_2 \rightarrow NCO + O} \quad (3)$$

In some experiments, $^{18}O_2$ was used to form isotopically labeled NC^{18}O:

$$\mathrm{CN + {}^{18}O_2 \rightarrow NC{}^{18}O + {}^{18}O} \quad (4)$$

Total rate constant and reaction products were measured by infrared laser absorption spectroscopy using lead salt diode lasers (Laser Components), as described in previous publications.[11,12] IR and UV light passed through a single-pass 143-cm absorption cell, and the infrared light was detected by a 1-mm diameter InSb detector (Cincinnati Electronics, ∼1 μs response time) and the signal was averaged on a digital oscilloscope. To account for small-probe laser thermal deflection affects, signals were collected with the diode laser slightly detuned off the spectroscopic absorption lines, and such transients were subtracted from the on-resonant transients. This is only a minor correction (<7%).

HCNO samples were synthesized as previously described by flash vacuum pyrolysis of 3-phenyl-4-oximino-isoxazol-5(4H)-one.[13−15] The purity of the HCNO samples was characterized by Fourier transform infrared (FTIR) spectroscopy and was typically 95% pure or better, with only small HNCO and CO_2 impurities detected. Because HCNO has poor long-term stability, samples were kept at 77 K except when filling the reaction cell. In general, HCNO could be allowed to stand at room temperature for ∼5 min in our Pyrex absorption cell with minimal decomposition.[2]

ICN (Aldrich) was purified by vacuum sublimation to remove dissolved air. O_2 (Matheson) and $^{18}O_2$ (Isotec) were passed through a glass column filled with Ascarite II to remove CO_2. SF_6 and CF_4 (Matheson) were purified by repeated freeze−pump−thaw cycles at 77 K and by passing through a glass column filled with Ascarite II.

The following molecules were probed using infrared diode laser absorption spectroscopy:

HCNO (0100^00^0) ← (0000^00^0)	R(10) at 2203.851 cm^{-1}
NCO ($v = 1 \leftarrow v = 0$)	at 1939.92 cm^{-1}
CO ($v = 1 \leftarrow v = 0$)	P (10) at 2103.27 cm^{-1}
NO ($v = 1 \leftarrow v = 0$)	R(8.5) at 1906.141 cm^{-1}

† Part of the special issue "James A. Miller Festschrift".
* Author to whom correspondence should be addressed.

10.1021/jp066036g CCC: $37.00
Published on Web 12/05/2006

CO_2 $(00^01) \leftarrow (00^00)$ P(32) at 2321.134 cm^{-1}

$^{16}O^{12}C^{18}O$ $(00^01) \leftarrow (00^00)$ P(13) at 2322.089 cm^{-1}

$^{18}O^{12}C^{18}O$ $(00^01) \leftarrow (00^00)$ R(12) at 2322.568 cm^{-1}

N_2O $(00^01) \leftarrow (00^00)$ P(23) at 2202.744 cm^{-1}

The HITRAN molecular database was used to locate and identify the spectral lines of NO, CO, CO_2, and N_2O product molecules.[16] Other published spectral data were used to locate and identify NCO[17] and HCNO[18] lines. The spectra lines used are near the peak of the rotational Boltzmann distribution, minimizing sensitivity to small heating effects.

Typical experimental conditions were P(HCNO) = 0.2 Torr, P(ICN) = 0.1 Torr, $P(O_2)$ = 4.0 Torr, $P(SF_6$ or $CF_4)$ = 1.5 Torr, and excimer laser pulse energies of 5 mJ. Under these conditions, we estimate an initial radical yield of $[CN]_0 \sim 1.8 \times 10^{13}$ molecule cm^3. CF_4 buffer gas was used for CO detection, while SF_6 buffer gas was used for detection of all other product molecules. The choice of buffer gas was motivated by the desire to relax any nascent vibrationally excited product molecules to a Boltzmann distribution.[19]

3. Results

3.1. Total Rate Constants. Figure 1 shows transient infrared absorption signals of the NCO radical, obtained with and without HCNO reagent. In the absence of HCNO reagent, an ~7000 s^{-1} decay rate over the time range 400 μs is observed. This decay is attributed to removal of NCO radicals by pathways other than the title reaction, including NCO + O and NCO + CN reactions as well as diffusion out of the probed region of the reaction cell. Upon the addition of HCNO reagent, a large increase in NCO decay rate is observed. Curves such as shown in Figure 1 were simulated by a single-exponential decay function. Figure 2 shows the resulting decay rates as a function of HCNO pressure. A linear dependence is observed, as is expected under the pseudo-first-order kinetics conditions, in which [HCNO] ≫ [NCO]. As per standard kinetic treatment, the slope of this plot is the desired bimolecular rate constant k_1:

$$k_1\,(298) = (1.58 \pm 0.20) \times 10^{-11}\ \text{cm}^3\ \text{molecule}^{-1}\ \text{s}^{-1}$$

The observed standard deviation (statistical error bar) was quite small, $\pm 0.05 \times 10^{-11}$ cm^3 $molecule^{-1}$ s^{-1}. The quoted error bar also includes an estimate of systematic errors, primarily on the basis of an estimate of the purity of the HCNO samples.

Attempts were made to measure the rate constant at temperatures both greater and lower than 298 K, unfortunately without success. At lower temperatures, the ICN precursor does not have sufficient vapor pressure to perform these experiments. At elevated temperatures, NCO absorption signals were weak and the data were quite scattered, possibly because of HCNO decomposition effects. The absorption coefficient of NCO is fairly low (much lower, for example, than CN), and the sensitivity of the infrared absorption probe decreases with increasing temperature because of increased Doppler line broadening, broadening of the rotational and vibrational Boltzmann distributions, and so forth.

3.2. Product Yields. Infrared diode laser absorption was used to attempt detection of NO, CO, CO_2, and N_2O products upon 248-nm photolysis of HCNO/ICN/O_2/buffer gas mixtures. Some transient signals are shown in Figure 3. All detection experiments were conducted at 298 K. A key point is that many of the same products produced by the title reaction may also be produced through 248-nm photolysis of HCNO and subsequent secondary chemistry. Possible chemistry involved was discussed in our previous publication.[2] To obtain product yields from the title reaction, product yields obtained from HCNO/O_2/buffer gas mixtures were subtracted from those obtained with the full HCNO/O_2/ICN/buffer gas mixtures. The assumption here is that the HCNO photolysis and secondary chemistry are not greatly affected by the presence or absence of the small amount of ICN precursor.

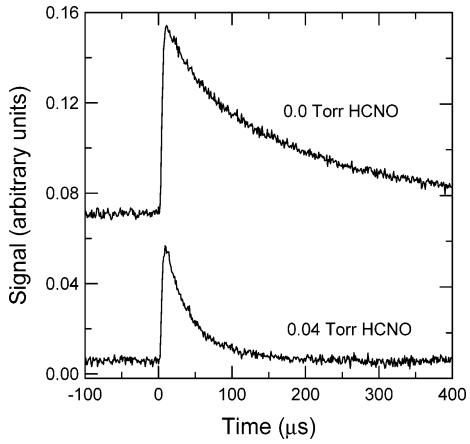

Figure 1. Diode infrared absorption signal of NCO as a function of time. Upper trace: 0.0 Torr HCNO; lower trace, 0.04 Torr HCNO. Reaction conditions: P(ICN) = 0.10 Torr, $P(O_2)$ = 4.0 Torr, $P(SF_6)$ = 1.0 Torr.

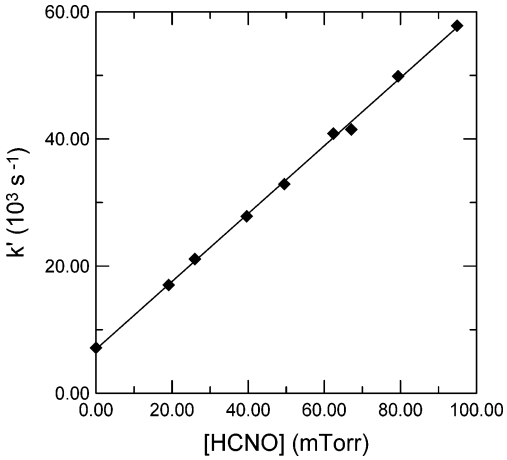

Figure 2. Pseudo-first-order decay rate constant of the NCO radical as a function of HCNO pressure. Reaction conditions: P(ICN) = 0.10 Torr, $P(O_2)$ = 4.0 Torr, $P(SF_6)$ = 1.0 Torr, P(HCNO) = variable.

We observed significant CO and NO transient signals upon photolysis of HCNO/O_2/ICN/SF_6. Much smaller CO and NO transient signals were obtained upon photolysis of HCNO/O_2/SF_6 mixture. This result suggests that channels 1a and possibly 1c represent significant product channels. A quantitative analysis (described below) will demonstrate that most or all of the CO products arise from 1a rather than from 1c.

CO_2 products from channel 1b are in principle easily detectable; however, a small CO_2 impurity in the HCNO samples interferes with this measurement. For that reason, and because of some other potential secondary chemistry, we used $^{18}O_2$ to produce isotopically labeled $NC^{18}O$ via eq 4. Reaction 1b, correspondingly, can be rewritten as follows:

$$NC^{18}O + HCNO \rightarrow {}^{16}OC^{18}O + HCNN \qquad (1b)$$

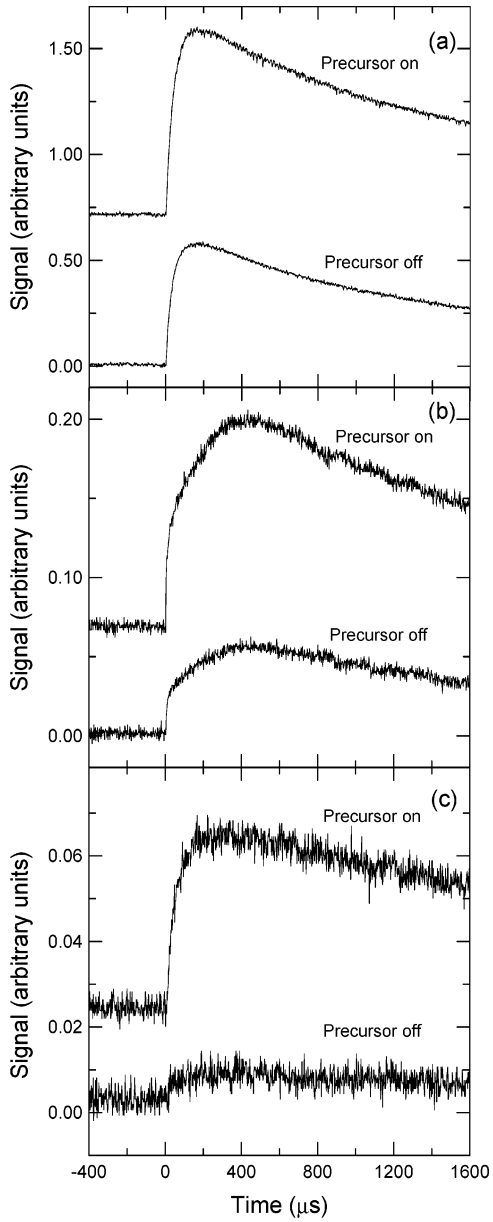

Figure 3. Transient infrared absorption signals of (a) CO, (b) NO, and (c) $^{16}OC^{18}O$. Reaction conditions: P(ICN) = 0 Torr (lower traces), P(ICN) = 0.10 Torr (upper traces), $P(O_2) = P(^{18}O_2)$, for $^{16}OC^{18}O$ detection only) = 4.0 Torr, P(HCNO) = 0.20 Torr, $P(CF_4)$ = 1.5 Torr (for CO transient only), $P(SF_6)$ = 1.5 Torr (for NO and $^{16}OC^{18}O$ transients only).

Therefore, the mixed isotope $^{16}OC^{18}O$ is expected to be produced from eq 1b when labeled oxygen is used. The experimental result is that we observed a significant $^{16}OC^{18}O$ transient signal upon photolysis of HCNO/ICN/$^{18}O_2$/SF_6 mixture while only a trace of $^{16}OC^{18}O$ transient signal was obtained upon photolysis of HCNO/$^{18}O_2$/SF_6 mixture, suggesting that 1b is a significant product channel.

No N_2O transient signal was observed upon photolysis of HCNO/ICN/O_2/SF_6. This demonstrates that channel 1d is not a product channel of the title reaction. We estimate an upper limit of the branching ratio $\varphi_{1d} < 0.02$.

Transient signal amplitudes (peak−peak) of NO, CO, and $^{16}OC^{18}O$ were converted into absolute concentration using HITRAN line strengths as described in a previous publication.[20] Table 1 shows a typical data set of product molecule yields. Shown are concentrations obtained both with and without the ICN precursor and the difference between these two measurements. The right-hand column of Table 1 shows the resulting relative product yields.

TABLE 1: Product Yields of Reaction NCO + HCNO[a]

product	without ICN[b]	with ICN[b]	difference[b,c]	relative yield[d]
NO	9.15	19.53	10.38	1
CO	13.73	24.55	10.82	1.042
$^{16}OC^{18}O$	0.081	0.559	0.478	0.046

[a] Experimental conditions: $P(O_2)$ = 4.0 Torr for detection of NO and CO, $P(^{18}O_2)$ = 4.0 Torr for detection of $^{16}OC^{18}O$, P(ICN) = 0.1 Torr, P(HCNO) = 0.2 Torr, and P(buffer gas) = 1.5 Torr. [b] In units of 10^{12} molecule cm^{-3}. [c] Obtained by subtracting column 3 by column 2. [d] Obtained from difference yields (column 4) being normalized to [NO] = 1.00.

Examination of Table 1 shows that the yields of NO and CO molecules are large and almost the same. This is consistent with NO and CO formation via channel 1a, with little or no contributions to these product yields from secondary chemistry. We therefore expect concurrent formation of HCN in channel 1a. HCN is not detectable in our diode laser apparatus because of the lack of available laser diodes near ~3300 cm^{-1}. However, FTIR spectra of both HCNO/ICN/O_2 and HCNO/O_2 mixtures before and after extensive photolysis (1000 excimer shots) clearly show that additional HCN products are produced from the photolysis of HCNO/ICN/O_2 mixture, beyond that formed by photolysis of HCNO/O_2. Although not a quantitative measurement, this result is consistent with our identification of channel 1a as a major product.

As shown in Table 1, only a trace of $^{16}OC^{18}O$ was produced upon the photolysis of a HCNO/$^{18}O_2$/SF_6 mixture, while a significant yield of $^{16}OC^{18}O$ yield was obtained by photolysis of a HCNO/ICN/$^{18}O_2$/SF_6 mixture. The difference between the two measurements represents the yield of CO_2 from eq 1b. However, this yield is much smaller than the yield of 1a, indicating that 1b is a relatively minor channel.

Table 1 shows nearly identical yields of CO and NO, suggesting that channel 1c is at most a minor channel. In addition, the possible presence of channel 1c can be tested by the following experiment. If $^{18}O_2$ is used to produce labeled $NC^{18}O$ radicals, the following reactions are expected:

$$NC^{18}O + HCNO \rightarrow C^{18}O + HC^{16}O + N_2 \qquad (1c)$$

$$HC^{16}O + {}^{18}O_2 \rightarrow C^{16}O + H^{18}O_2 \qquad (5)$$

or

$$NC^{18}O + HCNO \rightarrow C^{16}O + HC^{18}O + N_2 \qquad (1c)$$

$$HC^{18}O + {}^{18}O_2 \rightarrow C^{18}O + H^{18}O_2 \qquad (6)$$

Regardless of whether the oxygen-18 labeling ends up on the CO or HCO product in channel 1c, the reaction of the concurrently produced HCO radicals with oxygen guarantees that one molecule of $C^{16}O$ and one molecule of $C^{18}O$ are produced. The experiment result is that many more $C^{18}O$ molecules than $C^{16}O$ were detected upon photolysis of a HCNO/ICN/$^{18}O_2$/CF_4 mixture: a ratio of $[C^{18}O]/[C^{16}O] = 14$ was observed. This is clearly inconsistent with channel 1c and provides further evidence that most of the $C^{18}O$ originated from channel 1a. On the basis of our observed $[C^{18}O]/[C^{16}O]$ ratio, we estimate an upper limit of the branching ratio $\varphi_{1c} < 0.07$.

3.3. Secondary Chemistry. Two important possible secondary reactions merit discussion. The first is the reaction of oxygen atoms produced in eq 3 with HCNO:

$$O + HCNO \rightarrow HCN + O_2 \qquad \Delta H_{298}^0 = -285.27 \text{ kJ/mol} \quad (7a)$$

$$\rightarrow NCO + OH \qquad \Delta H_{298}^0 = -249.56 \text{ kJ/mol} \quad (7b)$$

$$\rightarrow CO + HNO \qquad \Delta H_{298}^0 = -431.36 \text{ kJ/mol} \quad (7c)$$

$$\rightarrow NO + HCO \qquad \Delta H_{298}^0 = -286.62 \text{ kJ/mol} \quad (7d)$$

Miller and co-workers used a large rate constant for the O + HCNO reaction in their modeling studies of NO-reburning,[1,21] but no experimental data or detailed theoretical calculations have been reported. Although a direct measurement of k_7 in our laboratory is not possible (we have no O-atom detection capabilities), we have attempted to detect products of eq 7 by infrared laser absorption upon 248-nm laser photolysis of HCNO/SO_2/buffer gas mixtures. Using experimental conditions of P(SO_2) = 0.3 Torr and 248-nm laser pulse energy of ~5 mJ, only a very small yield (~1.2×10^{12} molecule cm^{-3}) of CO was detected, and we were unable to detect NO in this experiment. Addition of O_2 (to convert HCO to CO) did not result in any detectable increase in the CO yield. This result is surprising, because under these experimental conditions, we estimate an initial O atom yield from SO_2 photolysis of ~1.8×10^{13} atom cm^{-3}, using the absorption cross section of SO_2 at 248 nm (8.78×10^{-20} cm^2).[22] Alternatively, we can experimentally determine $[O]_0$ by titrating O atoms with NO_2:

$$O + NO_2 \rightarrow NO + O_2 \quad (8)$$

Through detection of NO upon 248-nm laser photolysis of a NO/SO_2/SF_6 mixture, we obtained a yield of ~1.5×10^{13} atoms cm^{-3}, which is in excellent agreement with the value calculated from the SO_2 absorption coefficient.

As a result of the above experiment, one is tempted to conclude that 7c and 7d are at most minor channels. We can further deduce the products in 7b are also produced in very small amounts at most, because if OH were produced, it would react with HCNO to produce a significant yield of CO molecules.[2] These observations would tend to point to 7a as the major product. FTIR spectra of HCNO and HCNO/SO_2 mixtures before and after photolysis, however, showed no obvious differences that can be attributed to HCN formation via 7a. There are two possible explanations: perhaps 7a is the major channel, but the FTIR spectrum is not sufficiently sensitive to observe the HCN produced, primarily because of a large background signal from HCNO photolysis. Alternately, perhaps eq 7 is much slower than suspected at room temperature, which would explain our inability to detect any products in significant yield. Clearly, more study of eq 7 is warranted, but for the purposes of the present study, we can conclude that it does not represent a major interference while determining the products of eq 1.

The second potentially serious secondary reaction in our experiment is that of CN with HCNO. In a previous study in our laboratory, we found that this reaction is fast ($k_9 = 1.04 \times 10^{-10}$ cm^3 $molecule^{-1}$ s^{-1}) and has only one major product channel:[3]

$$CN + HCNO \rightarrow NO + HCCN \quad (9)$$

Equations 3 and 9 compete for CN radicals. In the limit of high O_2 pressure, eq 3 is expected to dominate. This is the reason for the large O_2 pressures used in most of the experiments reported here. One test of whether we have effectively shut down eq 9 is to use variable pressures of labeled $^{18}O_2$ (i.e., a HCNO/$^{18}O_2$/ICN/SF6 mixture is photolyzed). HCCN products of eq 9 then react with $^{18}O_2$ to produce doubly labeled $C^{18}O_2$:

$$HCCN + {}^{18}O_2 \rightarrow {}^{18}OC^{18}O + HCN \quad (10)$$

where $k_{10} = 1.8 \times 10^{-12}$ cm^3 $molecule^{-1}$ s^{-1} at 298 K.[23] CO_2 formed in eq 1b will be singly labeled, that is, $^{16}OC^{18}O$. Figure 4 shows the yield of $C^{18}O_2$ as a function of $^{18}O_2$ pressure. As expected, the yield becomes very small in the limit of high $^{18}O_2$, because most of the CN radicals react via 3 rather than 9 under these conditions. As shown in Table 2, at P($^{18}O_2$) = 4.0 Torr, we detected 2.37×10^{12} molecule cm^{-3} of $C^{18}O_2$ upon photolysis of a HCNO/$^{18}O_2$/ICN/SF_6 mixture but only 0.59×10^{12} molecule cm^{-3} $C^{18}O_2$ upon photolysis of a HCNO/$^{18}O_2$/SF_6 mixture. The difference between the two measurements is about ~1.8×10^{12} molecule cm^{-3}, representing the yield of $C^{18}O_2$ products from eqs 9 and 10. For comparison, we detected the yield of $C^{16}O_2$ and $^{16}OC^{18}O$ products along with $C^{18}O_2$ at P($^{18}O_2$) = 4.0 Torr, as shown in Table 2. From Table 2, we obtain the ratio of [$^{16}OC^{18}O$]/[$C^{18}O_2$] = 0.343. Combining this result with [$^{16}OC^{18}O$]/[NO] = 0.046 shown in Table 1, we obtain the ratio [$C^{18}O_2$]/[NO] = 0.134. According to the chemical equivalence relations in eqs 9 and 10, [$C^{18}O_2$] is equal to [NO] of eq 9. Equation 9, therefore, can account for approximately 13% of the total NO yield measured at P($^{18}O_2$) = 4.0 Torr. This is a rather minor yield and is comparable with effects of other secondary chemistry, such as O + HCNO. As a result, we conclude that the effect of eq 9 under the conditions reported in Table 2 is quite small.

In Figure 4, the yield of $C^{18}O_2$ decreases at high O_2 pressure but not quite to zero. One possible explanation may be a secondary reaction involving HCNN, produced by the minor channel 1b:

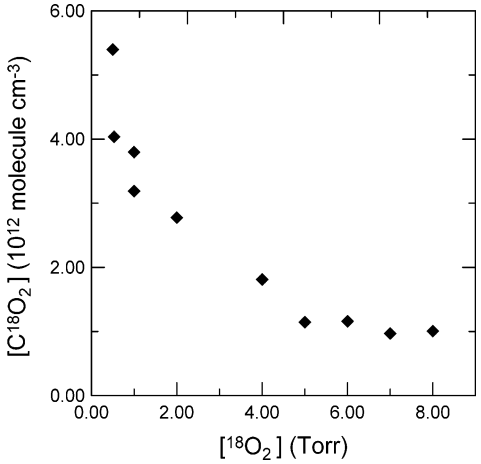

Figure 4. The dependence of $C^{18}O_2$ product yield on $^{18}O_2$ pressure. Reaction conditions: P(ICN) = 0.10 Torr, P(HCNO) = 0.20 Torr, P(SF_6) = 1.5 Torr, P($^{18}O_2$) = variable.

TABLE 2: Isotopically Labeled CO_2 Product Yields[a]

product	without ICN[b]	with ICN[b]	difference[b,c]	relative yield[d]
$C^{16}O_2$	0.447	0.572	0.125	0.067
$^{16}OC^{18}O$	0.106	0.719	0.613	0.343
$C^{18}O_2$	0.594	2.37	1.78	1

[a] Experimental conditions: P($^{18}O_2$) = 4.0 Torr, P(ICN) = 0.1 Torr, P(HCNO) = 0.2 Torr, P(SF_6) = 1.5 Torr. [b] In units of 10^{12} molecule cm^{-3}. [c] Obtained by subtracting column 3 by column 2. [d] Obtained from difference yields (column 4) being normalized to [$C^{18}O_2$] = 1.00.

$$HCNN + {}^{18}O_2 \rightarrow C^{18}O_2 + N_2 + H \qquad \Delta H_{298}{}^{0} = -635.23 \text{ kJ/mol} \quad (11)$$

(other product channels may also be possible). No study of this reaction has been reported in the literature. Equation 11 does not affect our determination of φ_{1b}, which is based on measurement of [$^{16}OC^{18}O$] yields.

In summary, we can conclude that channel 1a dominates the title reaction but that a small yield of 1b exists as well. On the basis of the quantitative data and after consideration of the uncertainties present, we estimate $\varphi_{1a} = 0.92 \pm 0.04$ and $\varphi_{1b} = 0.04 \pm 0.02$.

4. Discussion

Our results represent the first study of the title reaction. Several experimental artifacts can cause systematic errors in a pseudo-first-order kinetics experiment. The first, decomposition of HCNO sample during the experiments, was minimized by completing a single NCO IR transient signal decay measurement in about 5 min (typically, this allows 2 min for filling the cell and 3 min for the reagents to mix). In this amount of time, less than 10% decomposition occurs. A related issue is the possible reaction of NCO radicals with decomposition products and reaction products from the title or secondary reactions. This issue was discussed in our previous publications[2,3] and was shown to be insignificant when the measured rate constant of the title reaction is fast, as is the case here. If k_1 were several orders of magnitude slower, such secondary chemistry would be a more serious issue.

One notable feature of the absorption signals shown in Figure 1 is that the NCO peak transient amplitude is decreased when HCNO is included in the reaction mixture. This is partly because in the lower trace of Figure 1, the decay rate is almost as fast as the rise rate; an extrapolation of the decay to $t = 0$ would yield a substantially increased amplitude. Additional reasons for this effect include competition for CN radicals (eq 3 vs eq 9) as well as a slight amount of decomposition of ICN in the presence of HCNO.

No ab initio studies of the potential energy surface of this reaction have been reported. We can therefore only speculate regarding details of the reaction mechanism. Our observation of channel 1a as the major product channel suggests the following possible mechanisms: NCO attack at the carbon of HCNO forms a HC(NCO)NO complex, which dissociates via N−C bond fission to produce a CO molecule and via a further C−N bond fission to produce NO and HCN products. Alternatively, NCO attacks the oxygen of HCNO to form a quasi-linear complex HCNONCO, followed by fission of the first N−O bond and second N−C bond to produce HCN, NO, and CO products. Both of these mechanisms are consistent with our observation that the CO formed upon photolysis of HCNO/ICN/$^{18}O_2$/SF_6 mixture is primarily the $C^{18}O$ isotope.

5. Conclusion

The kinetics and products of NCO + HCNO reaction were studied using IR diode laser absorption spectroscopy. The reaction is fast, with $k_1 = (1.58 \pm 0.20) \times 10^{-11}$ cm^3 molecule^{-1} s^{-1} at 298 K. The major product channel is NO + CO + HCN.

Acknowledgment. This work was supported by Division of Chemical Sciences, Office of Basic Energy Sciences of the Department of Energy, Grant DE-FG03-96ER14645. Partial support from ND EPSCoR through NSF grant #EPS-0447679 is also acknowledged.

References and Notes

(1) Miller, J. A.; Klippenstein, S. J.; Glarborg, P. *Combust. Flame* **2003**, *135*, 357.
(2) Feng, W.; Meyer, J. P.; Hershberger, J. F. *J. Phys. Chem. A* **2006**, *110*, 4458.
(3) Feng, W.; Hershberger, J. F. *J. Phys. Chem. A.*, accepted for publication.
(4) Perry, R. A.; Siebers, D. L. *Nature* **1986**, *324*, 657.
(5) Miller, J. A.; Bowman, C. T. *Int J. Chem. Kinet.* **1991**, *23*, 289.
(6) Siebers, D. L.; Caton, J. A. *Combust. Flame* **1990**, *79*, 31.
(7) Chase, M. W. NIST-JANAF Thermochemical Tables. *J. Phys. Chem. Ref. Data*, 4th ed. **1998**.
(8) Schuurman, M. S.; Muir, S. R.; Allen, W. D.; Schaefer, H. F., III. *J. Chem. Phys.* **2004**, *120*, 11586.
(9) Clifford, E. P.; Wenthold, P. G.; Lineberger, W. C.; Petersson, G. A.; Broadus, K. M.; Kass, S. R.; Kato, S.; Depuy, C. H.; Bierbaum, V. M.; Ellison G. B. *J. Phys. Chem. A* **1998**, *102*, 7100.
(10) Osborn, D. L.; Mordaunt, D. H.; Choi, H.; Bise, R. T.; Neumark, D. M.; Rohlfing, C. M. *J. Chem. Phys.* **1997**, *106*,10087.
(11) Cooper, W. F.; Hershberger, J. F. *J. Phys. Chem.* **1992**, *96*, 771.
(12) Cooper, W. F.; Hershberger, J. F. *J. Phys. Chem.* **1992**, *96*, 5405.
(13) Pasinszki, T.; Kishimoto, N.; Ohno, K. *J. Phys. Chem.* **1999**, *103*, 6746.
(14) Wentrup, C.; Gerecht, B.; Briehl, H. *Angew. Chem., Int. Ed. Engl.* **1979**, *18*, 467.
(15) Wilmes, R.; Winnewisser, M. *J. Labelled Compd. Radiopharm.* **1993**, *33*, 157.
(16) Rothman, L. S.; et al. *J. Quant. Spectrosc. Radiat. Transfer* **1992**, *48*, 469.
(17) Brüggemann, R.; Petri, M.; Fishcer, H.; Mauer, D.; Reinert, D.; Urban, W. *Apply. Phys. B* **1989**, *48*, 105.
(18) Ferretti, F. L.; Rao, K. N. *J. Mol. Spectrosc.* **1974**, *51*, 97.
(19) Cooper, W. F.; Hershberger, J. F. *J. Phys. Chem.* **1992**, *96*, 771.
(20) Cooper, W. F.; Park, J.; Hershberger, J. F. *J. Phys. Chem.* **1993**, *97*, 3283.
(21) Miller, J. A.; Durant, J. L.; Glarborg, P. *Proc. Combust. Inst.* **1998**, *27*, 234.
(22) Wu, C. Y. R.; Yang, B. W.; Chen, F. Z.; Judge, D. L.; Caldwell, J.; Trafton, L. M. *Icarus* **2000**, *145*, 289.
(23) Adamson, J. D.; Desain, J. D.; Curl, R. F.; Glass, G. P. *J. Phys. Chem. A* **1997**, *101*, 864.